Modulation of Coherently Coupled Phased Photonic Crystal Vertical Cavity Laser Arrays

Stewart T. M. Fryslie, *Student Member, IEEE*, Zihe Gao, *Member, IEEE*, Harshil Dave, *Member, IEEE*, Bradley J. Thompson, *Member, IEEE*, Katherine Lakomy, *Student Member, IEEE*, Shiyun Lin, Patrick J. Decker, *Member, IEEE*, David K. McElfresh, *Member, IEEE*, José E. Schutt-Ainé, *Fellow, IEEE*, and Kent D. Choquette, *Fellow, IEEE*

(Invited Paper)

***Abstract*—The modulation properties of two-element photonic crystal ion-implanted coherently coupled vertical cavity surface emitting laser arrays emitting at 850 nm are reported. Single mode emission into either the in-phase or out-of-phase supermode and significant modulation bandwidth enhancement are obtained for both operating conditions. We model our device as a monolithically integrated, mutually optically injection-locked laser system and show that the phase detuning and injection ratio between array elements are critical parameters influencing modulation bandwidth. Comparison of our experimental measurements to our model is consistent with mutual injection locking. Modulation bandwidth greater than 30 GHz and up to 37 GHz is consistently found for several array designs. We show the modulation response can be tailored for different applications.**

***Index Terms*—Phased arrays, semiconductor laser arrays, vertical cavity surface emitting lasers (VCSELs).**

I. Introduction

THE effects of optically coupling two or more semiconductor lasers have been explored for more than four decades [1]. These prior studies include investigation of the interaction between discrete laser diode sources as well as the interaction between laser elements of monolithic laser arrays. There have been several different perspectives used in the analysis of optical coupling between semiconductor lasers, which include injection locking to study temporal dynamics [2], as well as emission supermodes derived from coupled-mode theory to characterize spatial coherence [3], [4]. Vertical cavity surface emitting lasers (VCSEL) are interesting candidates for optically coupled arrays, and both injection-locking, as well as supermode analysis have been separately explored.

The majority of prior injection-locking VCSEL studies have used an external VCSEL or other laser source to lock another VCSEL to increase its modulation bandwidth [5]–[9]. The injection-locking results have been successfully modelled using a rate equation approach to account for the effects of the magnitude of the injected field as well as frequency detuning between the VCSELs [2]. Dramatic modulation bandwidth increase to 50 GHz was demonstrated for a 1.55 μm VCSEL under extremely high optical intensity injection conditions [7]. Two-dimensional VCSEL arrays as large as 5×5 have also been successfully externally injection-locked to operate in the coherent low divergence in-phase super mode [10].

A supermode analysis of 2-dimensional VCSEL arrays identified the in-phase (out-of-phase) supermodes with an on-axis far-field intensity maximum (null), respectively [11]. The out-of-phase mode arises when the fields of the adjacent elements in the VCSEL array have a π -phase difference. More recently we have studied 1- and 2-dimensional VCSEL arrays and have shown that arbitrary phase difference between array elements is possible [12]. Further, the phase can be controlled by an independent bias applied to each element, which enables continuous 2-dimensional beam steering [13], [14].

VCSELs are widely deployed as low-cost high performance laser sources for fiber optic data transmission in computer servers, data centers, supercomputers, and throughout the internet. The modulation bandwidth for free-running VCSELs typically ranges from ten to twenty GHz. An interesting discovery is that the modulation bandwidth can be appreciably improved in coherently coupled VCSEL arrays [15]–[17]. Dalir and Koyama have reported 30 Ghz bandwidth [15] and as high as 36 Gbps data rate [16] from dual optically coupled oxide-confined VCSELs. We have previously reported small signal bandwidth as high as 37 GHz using a two-element coherent VCSEL array [17]. Moreover, we have shown that electroni-

Manuscript received February 1, 2017; revised April 25, 2017; accepted April 26, 2017. Date of publication April 28, 2017; date of current version July 11, 2017. This work was supported in part by the National Science Foundation under Award No. 15-09845 and Oracle Corporation, Redwood, CA, USA. *(Corresponding author: Zihe Gao.)*

S. T. M. Fryslie was with the Department of Electrical and Computer Engineering, University of Illinois at Urbana-Champaign, Champaign, IL 61801 USA. He is now with the Freedom Photonics LLC, Santa Barbara, CA 93117 USA (e-mail: fryslie2@illinois.edu).

Z. Gao, H. Dave, B. J. Thompson, K. Lakhomy, J. E. Schutt-Ainé and K. D. Choquette are with the Department of Electrical and Computer Engineering, University of Illinois at Urbana-Champaign, Champaign, IL 61801 USA (e-mail: zihegao2@illinois.edu; hdave5@illinois.edu; thomps12@illinois.edu; lakomy2@illinois.edu; jesa@illinois.edu; choquett@illinois.edu).

P. Decker, S. Lin, and D. K. McElfresh are with the Oracle Corporation, Redwood City, CA 94065, USA (e-mail: patrick.decker@oracle.com; shiyun.lin@Oracle.com; david.mcelfresh@oracle.com).

Color versions of one or more of the figures in this paper are available online at http://ieeexplore.ieee.org.

Digital Object Identifier 10.1109/JSTQE.2017.2699630

cally tunable phase tuning between two coupled VCSELs can lead to various conditions of coherently coupled operation [18].

In this paper we report theory and modulation measurements of two-element coherently-coupled implant-defined photonic crystal VCSEL arrays emitting nominally at 850 nm. The two strongly optically-coupled VCSELs in the array are modeled as monolithic mutual injection-locked lasers based on the well established injection-locking laser rate equations [2]. We have designed and fabricated optically coupled and electrically isolated 1×2 VCSEL arrays emitting at 850 nm and have developed an operation procedure where bias conditions are leveraged to control the index profile and coupling phase for optimum modulation bandwidth. Experimentally we demonstrate modulation bandwidth enhancement for both in-phase and out-of-phase operation to as high as 37 GHz, as well as 25 Gbps data rate, both limited by our experimental setups.

We first describe the design for achieving single supermode operation in photonic crystal VCSEL arrays, as well as our fabrication approach based entirely on conventional processing which allows for independent phase tuning of the array elements. Next we present the injection-locking model, where we have explicitly incorporated the relative phase between the array elements. In the analysis section, we compare our modeling and measurement results to analyze various dynamic phenomena. We finally summarize the high speed modulation performance and report several device designs that achieve bandwidth in excess of 30 GHz in single transverse mode operation.

II. Design and Fabrication of Phased VCSEL Arrays

Transverse electrical and optical confinement are critical in VCSEL and VCSEL array designs for achieving high efficiency or low threshold current. While oxide-confined VCSELs have dominated the short-haul optical interconnect market due to low threshold current, high power conversion efficiency, and high modulation bandwidth, they typically emit into multiple transverse modes due to the inherent large index contrast [19]. Decreasing the size of the oxide aperture can eliminate the higher order modes, but at the cost of increasing the series resistance and current density, hence degrading VCSEL reliability. This dilemma motivated our research efforts on ion-implanted photonic crystal VCSELs [20], where electrical and optical confinement are separately provided by proton-implantation and photonic crystal patterns, respectively. The photonic crystal, consisting of periodic pattern of air holes etched into the top distributed Bragg reflector, provides optical confinement that is controlled by the photonic crystal pattern, hole separation b, hole diameter a, and hole etch depth. Holes missing from the photonic crystal pattern create the optical cavities of the array elements. The index difference is chosen to be around 10^{-3}, which implies only a few to a single transverse mode are confined. For the coupled arrays, we use similar photonic crystal designs that provided single transverse mode emission [21], but incorporate two or more missing holes to delineate two or more elements within the coupled VCSEL array [22]–[26].

Coherently coupled photonic crystal VCSEL arrays were initially fabricated by simply having multiple defects (missing holes) adjacent to each other [22]. Modifying the size and position of the near-element holes was shown to influence the coupling properties and promote in-phase coupling [24]. Furthermore, by coupling through the gap between the holes and/or eliminating the inter-element holes, the index guiding between elements is suppressed. Moreover, due to the electronic suppression of the index in each element during current injection, the arrays are antiguided, since the refractive index between elements is higher than in the individual laser optical apertures [26]. With properly designed inter-element spacing, the antiguided photonic crystal arrays can operate in-phase consistently for arrays as large as 3×3 [27], [28].

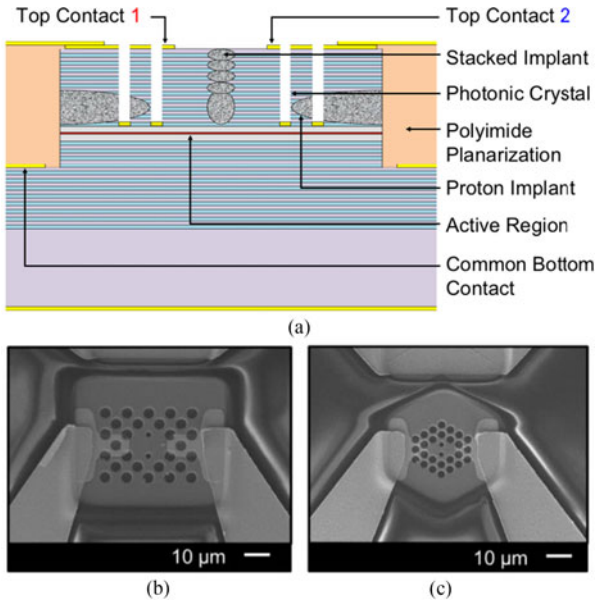

Fig. 1. (a) Cross-sectional sketch and (b) and (c) scanning electron micrographs of 1×2 optically coupled, phased vertical cavity laser array. The array in (b) has square-lattice with $b = 3.6\,\mu$m and $b/a = 0.6$ and the array in (c) has hexagonal-lattice with $b = 2.4\,\mu$m and $b/a = 0.6$.

Fig. 1 shows a side view sketch and images of square and hexagonal photonic crystal designs for 2×1 arrays. The size of ion-implantation gain aperture is chosen to be slightly larger than the optical aperture to insure relatively low series resistance [20]. The use of ion implantation to independently define the gain aperture of each element means that relatively low current density can be maintained. Electrical isolation between the elements is important to allow independent current injection into each element. As shown in Fig. 1(a), multiple ion implant steps with varying acceleration ion energies were done between the elements to create stacked implant damage to the top surface [29].

A fabrication challenge for multiple element ion-implanted photonic crystal VCSEL arrays is non-uniformity among the elements of the array caused by fabrication imperfections [28]. In arrays where all the elements share the same electrode, this variation leads to differing series resistance, and thus the current is unequally divided among the elements. The result is spectral detuning among the array elements, which will degrade the array coherence. This can be overcome by individually controlling the injection current into each element, which allows tuning the array into coherence [18].

In addition to forcing the elements in the phased VCSEL array to spectrally align, the ability to control injected currents to individual array elements has enabled other aspects of coherent VCSEL arrays, including high-speed beam steering up to 100 MHz [30] based on phase or wavelength detuning [31], observation of gain tuning and parity-time symmetry breaking [32], and modulation bandwidth enhancement [17]. The latter aspect is the focus of this paper. As indicated in Fig. 1, each array has two anode contacts, one to each element, with low capacitance contact pads on polyimide in a ground-signal-signal-ground geometry for high speed on-wafer probing.

III. Modeling of Coherent VCSEL Arrays

We model the coupled two-element photonic crystal VCSEL array as a monolithically integrated, mutually optically injection-locked laser system. The master laser array element is modeled as a single-mode laser, with a contribution of optical feedback originating from the slave laser array element. This is achieved using the single-mode injection locking rate equations without an isolator [33]–[36], written in terms of the normalized complex field envelope E_m,

$$\frac{dE_m}{dt} = \frac{1}{2}(1+j\alpha)\left[g(N_m - N_{tr}) - \frac{1}{\tau_p}\right]\cdot E_m + \kappa E_{inj,s} e^{j\Psi}$$

where $E_{inj,s}$ is the injected field from the slave laser array element, g is linear gain coefficient, α is semiconductor linewidth enhancement factor, N_m is carrier number, N_{tr} is transparency carrier number, τ_p is photon lifetime, κ is coupling coefficient, and Ψ is the preferential phase of the coupled mode, being 0 or π for the in-phase or out-of-phase coupled mode, respectively. The frequency detuning between master and slave laser array elements is set to zero since the feedback will be at the same wavelength as the master laser.

Similarly, the slave laser array element is modeled as having strong optical injection from the master laser array element [33], with complex field rate equation given by,

$$\frac{dE_s}{dt} = \frac{1}{2}(1+j\alpha)\left[g(N_s - N_{tr}) - \frac{1}{\tau_p}\right]\cdot E_s + \kappa E_{inj,m} e^{j\Psi} - j2\pi\Delta f_{inj} E_s$$

where $E_{inj,m}$ is the injected field from the master laser array element and Δf_{inj} is the detuning frequency defined as the difference between the locked frequency of the coupled mode f_C and the free-running laser element frequency f_{fr} : $\Delta f_{inj} \equiv f_C - f_{fr}$. Writing these equations in terms of the photon numbers and phase gives the well-known injection-locked laser coupled rate equations for photon density, phase, and carrier number. For the slave laser, these are

$$\frac{dS_s}{dt} = \left[g(N_s - N_{tr}) - \frac{1}{\tau_p}\right]\cdot S_s + 2\kappa\sqrt{S_{inj,m}S_s}\cos(\phi_s)$$

$$\frac{d\phi_s}{dt} = \frac{\alpha}{2}\left[g(N_s - N_{tr}) - \frac{1}{\tau_p}\right] - \kappa\sqrt{\frac{S_{inj,m}}{S_s}}\sin(\phi_s) - 2\pi\Delta f_{inj}$$

$$\frac{dN_s}{dt} = J_s - \frac{1}{\tau_n}N_s - g(N_s - N_{tr})\cdot S_s$$

TABLE I
List of Simulation Parameters

Symbol	Parameter	Value	Units
–	Wavelength	850	nm
L	Length of cavity	1×10^{-4}	cm
–	Length of active region	24×10^{-7}	cm
–	Reflectivity of output mirror	0.998	–
τ_n	Carrier lifetime	2	ns
τ_p	Photon lifetime	2×10^{-3}	ns
g	Linear gain coefficient	2×10^{-16}	cm^2
–	Optical confinement factor	0.043	–
n_{tr}	Transparency carrier number	5.23×10^{18}	#
–	Operating current	$4 \times I_{th}$	mA
I_{th}	Threshold current	2	mA
α	Linewidth enhancement factor	4	–
–	Injection coupling rate	802	1/ns

where S_s is photon number, J_s is current number, and N_s is carrier number, and ϕ_s is the phase detuning defined as the difference between slave and master taking into account the coupled mode phase: $\phi_s \equiv \phi_{slave} - \phi_{master} - \Psi$. Due to the leaky nature of the anti-guided coupling mechanism, the electromagnetic field in the inter-element coupling region has real propagation vectors and shows standing wave patterns. An odd number of inter-element intensity maxima corresponds to in-phase operation and even number for out-of-phase operation [26], [37], [38]. The published values of κ for injection locked VCSELs vary greatly, from 1.0×10^{11} to 5.0×10^{13} [39], and the coupling coefficient is in general a complex number with its phase varying with the inter-element spacing [40], [41]. For our analysis we use a value of 8.02×10^{11} as taken from [42]. The modulation response of the injection locked laser array element can be simulated using small signal analysis. However, doing so requires that we designate one array element as the master and the other array element as the slave. Stability analysis gives us the phase (wavelength) detuning boundaries of the stable locking range for an injection locked laser [43], [44]. Solving the coupled rate equations for the steady-state values of photon number, phase, and carrier number, the requirements for real phase and stable gain give constraints on the phase (wavelength) detuning for injection locking [43]. This constraint is known as Mogensen's locking range and given by

$$-\frac{\pi}{2} \le \phi \le \cot^{-1}\alpha$$

$$-\kappa\sqrt{\frac{S_{inj,m}}{S_s}}\sqrt{1+\alpha^2} \le 2\pi\Delta f_{inj} \le -\kappa\sqrt{\frac{S_{inj,m}}{S_s}}$$

which is of course related to wavelength detuning by $\Delta\lambda_{inj} = (c/f_0) - (c/(f_0 - \Delta f_{inj}))$ Further constraints on the stable portion of the locking range for frequency response are imposed by the dynamic equation solutions for the frequency response to remain stable [43], [44].

Using the small signal analytic model we can simulate the small signal frequency response across the entire locking range. The various laser parameters required for simulation are given in Table I and are either calculated or typical values for 850 nm VCSELs are used [45]. The borders of the map are created by

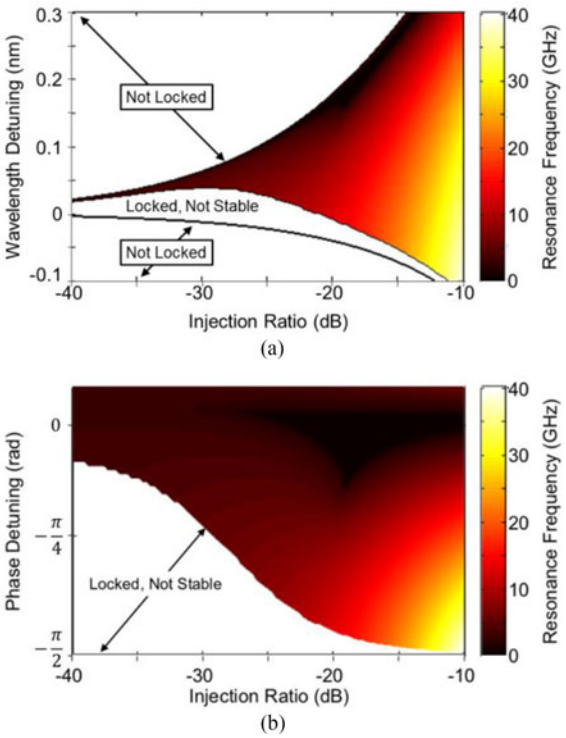

Fig. 2. Simulated maps of the locking range showing modulation response resonance frequency vs. injection ratio and (a) spectral resonance wavelength detuning or (b) relative coupling phase detuning for one element being injection locked by another.

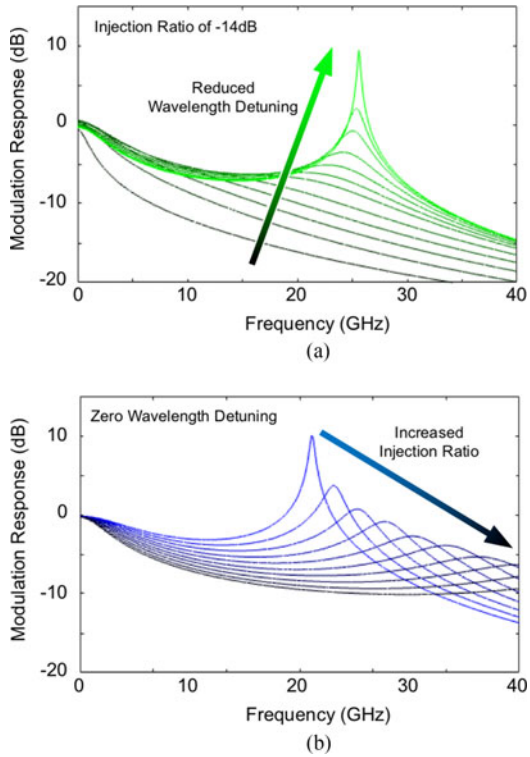

Fig. 3. Simulated modulation response curves for (a) decreasing value of wavelength or phase detuning at a fixed injection ratio and (b) increasing injection ratio at a fixed wavelength detuning of zero, for one element being injection locked by another.

stability analysis [43], [44] while the response is calculated by small signal analysis [33], [35], [39], [46], [47]. The plots in Fig. 2 show the resonance frequency for the simulated stable locked regions of the array. In the plots of Fig. 2, the abscissa is the injection ratio, while the ordinate is either the wavelength or phase detuning between the array elements. The color scale corresponds to the resonance frequency of the modulation response. Fig. 2 shows the general trend that the resonance frequency increases with injection ratio and reduced wavelength (phase) detuning value. The locking range maps are useful in developing device designs as well as operating procedures to induce a desired response, and have been thoroughly analyzed for injection locked lasers [33], [35], [36], [39], [42]–[44], [46]–[51].

The effect of phase (wavelength) detuning at a fixed injection ratio for the resonance frequency is shown in Fig. 3(a). The response has a high frequency resonance peak at the low phase (wavelength) detuning end of the locking range, whereas it is highly damped without resonance peak at the high detuning end. Low bandwidth applications requiring high linearity may benefit from the response at the high detuning end, whereas high frequency and narrow-band applications such as RF photonic link technology may benefit from the response at the low detuning end.

The effect of increasing field injection while the wavelength detuning is held at zero for the resonance frequency is shown in Fig. 3(b). The response becomes more damped as the injection ratio is increased, and produces a large 3-dB bandwidth. This is the ideal behavior for optical communications applications requiring large broadband 3-dB bandwidth. Not only is this behavior the most desirable but, as we will show, also the most likely to be produced by the coherently coupled VCSEL arrays. As will be shown in the following section, the spectral detuning for the array elements when under coherently coupled operation are very near zero, and by manipulation of the field distribution large injection ratios can be achieved.

IV. Analysis

As shown by the theoretical analysis of the previous section, the modulation response performance depends on the field injection ratio and phase (or wavelength) detuning between the two elements while locked. In this section we analyze the qualitative agreement between experimental data and locking range dynamics based on mutual injection locking theory.

To analyze the effects of phase (wavelength) detuning on the modulation response, we use the experimental data presented in Figs. 4–6 from a square-lattice photonic crystal VCSEL array with $b = 3.3\,\mu$m and $b/a = 0.6$. The current injected into the array elements are denoted as I_1 and I_2. The spectral data in Fig. 4 shows that for constant $I_1 = 5.1$ mA, the array becomes coherently coupled for I_2 varying between 3.8 to 5.1 mA. Measurements of the far-field intensity profile and spectral behavior confirm that the array lases in the out-of-phase coupled mode. As predicted by coupled mode theory and demonstrated in Fig. 4, the out-of-phase mode prefers higher frequency and the coupled array lases at a wavelength near the natural resonance of

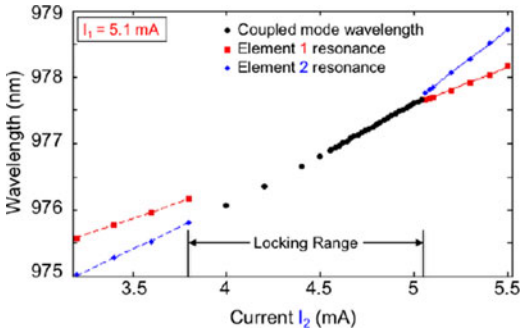

Fig. 4. Spectral data showing resonance wavelength vs. bias currents ($I_1 = 5.1$ mA while I_2 is varied) for fundamental modes of elements 1 (red square) and 2 (blue diamond) and the coupled mode (black circles) through locking range.

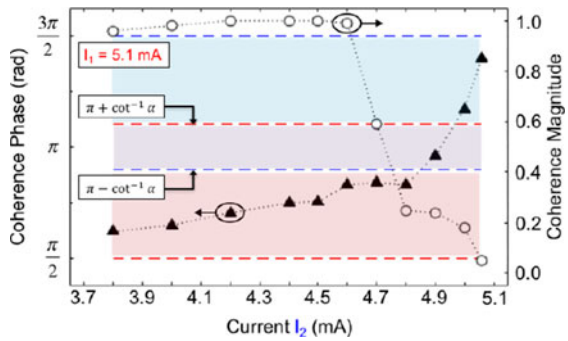

Fig. 5. Coherence phase (triangle) and magnitude (circle) extracted via near- and far-field analysis. Phase constraints of injection locking for Element 1 and Element 2 are indicated with red and blue, respectively, dashed lines and shading.

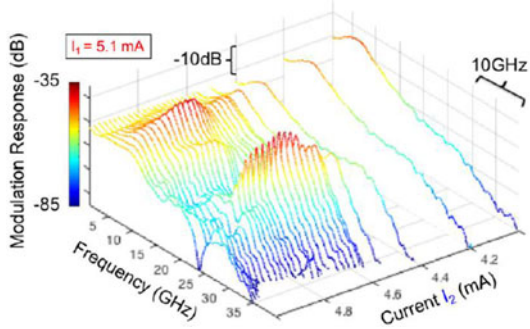

Fig. 6. Modulation response vs. bias currents ($I_1 = 5.1$ mA while I_2 is varied) throughout the locking range.

whichever element is blue-detuned. Therefore, the wavelength detuning between the natural resonance of at least one element and the coupled mode wavelength is very near zero detuning throughout the locking range (e.g. the wavelength detuning is near zero for Element 2 through most of the locking range in Fig. 4).

For an array element to be injection locked, its phase relative to that of the other element must satisfy $\pi/2 \leq \phi \leq (\pi + \cot^{-1}\alpha)$ for the out-of-phase coupled mode. Note that further constraints are imposed by the dynamic equation solutions for the frequency response to remain stable. By propagating the experimentally determined near-field apertures to the far-field via the Fraunhofer approximation such that the propagated profile closely matches the experimentally determined far-field intensity profile, we may extract the phase detuning and coherence magnitude of the laser array [31]. The results are plotted in Fig. 5 where the shaded regions of the plot indicate phase relationships for which Element 1, Element 2, and both elements, respectively, satisfy the phase conditions to be injection locked. Note that the absolute values of phase are subject to the alignment of the equipment when the data is collected, but that relative phase change across the locking range should be accurate.

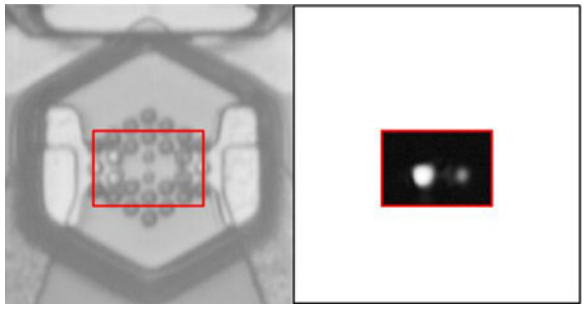

Fig. 7. Micrographs of (left) hexagonal-lattice VCSEL array with $b = 2.7$ μm and $b/a = 0.6$ and (right) near-field intensity with the left element having $I_1 = 7.9$ mA and the right element having $I_2 = 6.8$ mA and small signal modulation applied.

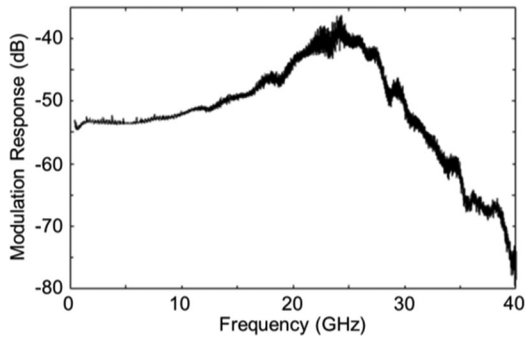

Fig. 8. Modulation response at the bias conditions in Fig. 7.

The modulation response at bias conditions throughout the locking range for various currents are shown by Fig. 6. In this plot, the modulation response shows the lack of an enhanced resonance peak when phase conditions are met for Element 1 to be injection locked ($I_2 \leq 4.5$ mA), whereas there is a clear enhanced modulation response resonance peak at 25 GHz for bias at which the near-zero-wavelength-detuned Element 2 has relative phase satisfying the conditions for being injection locked ($4.6\,\text{mA} < I_2 < 4.9\,\text{mA}$). This shows qualitative agreement between experimental data and the theory of mutual injection locking. By comparing the modulation response in Fig. 6 with the coherence magnitude in Fig. 5, we see also that the magnitude of modulation response at mid-frequencies (10 to 20 GHz) reduces with decreasing coherence magnitude. This behavior has been observed for multiple arrays.

To analyze the effects of field injection ratio on the modulation response, we use the experimental data in Figs. 7 and 8 from a hexagonal-lattice photonic crystal VCSEL array with $b =$

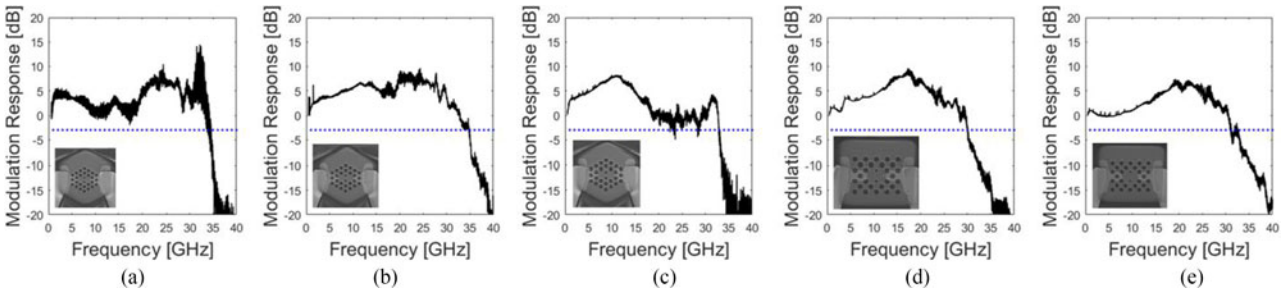

Fig. 9. Small signal modulation response showing 3-dB bandwidth beyond 30 GHz for devices with each of five photonic crystal designs on sample. A scanning electron micrograph of the corresponding device is shown by the inset.

2.7 μm and $b/a = 0.6$. The array shown in Fig. 7 is biased with DC currents of $I_1 = 7.9$ mA and $I_2 = 6.8$ mA. In Fig. 7, this corresponds to the right Element 2 in an injection-locked state with significantly lower field amplitude than for the left Element 1, which has brighter intensity in the near-field inset. We apply small signal modulation to Element 2 in order to take full advantage of the effects of this asymmetric field distribution. This gives the relatively flat 3-dB bandwidth of 33 GHz shown in Fig. 8, which lacks the peak in low frequency gain (e.g. Fig. 6) typically observed when the field distribution is more symmetric.

The peak in the low frequency gain of the typical response, when both elements lase with similar field distribution, is caused by the master laser either being directly modulated by an electrical signal (if the small signal modulation is applied to the master) or being modulated by optical feedback due to the field of the slave being coupled to it. When the field amplitude being coupled into the master from the modulated slave is significantly less, it has reduced effect on the light output from the master [35]. Therefore, the response from direct modulation of the slave laser will be relatively flat, without low frequency gain from modulation of the master laser. Additionally, the modulation response should have a large 3-dB bandwidth enhancement due to larger field injection ratio for the coupled element with less field amplitude.

This indicates an operating procedure to achieve broadband modulation response that is relatively flat over a large frequency range: induce field distribution asymmetry (through either bias conditions or cavity design) and modulate the element with lower field amplitude in an injection-locked state.

V. High-Speed Performance

Previously, we reported record high modulation bandwidth of 37 GHz with narrow spectral width emission at 980 nm wavelength from an array operating in the out-of-phase coupled mode [17]. We demonstrate in Fig. 9 that several arrays of different design, all emitting nominally at the 850 nm wavelength, are capable of bandwidth enhancement beyond 30 GHz. The small signal responses in Fig. 9 are not particularly flat and narrow resonances can sometimes be seen, in agreement with other reports [52], [53]. Nevertheless, photonic crystal VCSEL arrays are capable of large signal modulation as well. Fig. 10 shows the small signal bandwidth as well as the eye pattern for 25 Gb/s

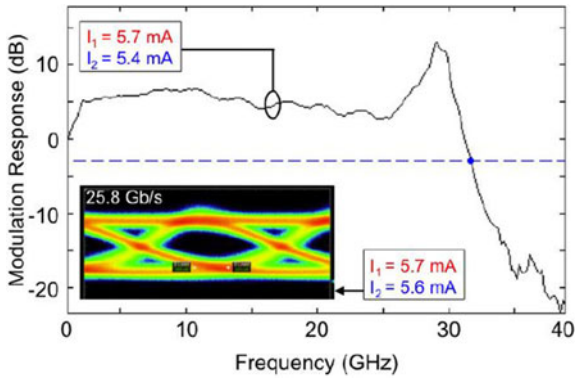

Fig. 10. Small signal response and inset eye-diagram showing open eyes at 25 Gb/s data rate.

data rate for an array under nearly identical bias conditions. Both measurements were limited by the testing equipment. Together, the performance demonstrated in Figs. 9 and 10 shows that coherently coupled photonic crystal VCSEL arrays are capable of enhanced modulation response suitable for optical communications applications.

The 2 $\times$ 1 photonic crystal coherent VCSEL arrays used in Ref. [17] employed a focused ion beam etch (FIBE) for current isolation between array elements, whereas those of Fig. 9 employed a stacked ion implantation step as previously discussed. The FIBE-induced optical loss between array elements will tend to pin the supermode null of the electric field such that the out-of-phase coupled mode is preferred. The out-of-phase on-axis null in the far-field intensity profile and is undesirable for coupling the array emission to optical fiber. All previous reports of bandwidth enhancement from coupled VCSEL arrays has occurred for out-of-phase coupling [15]–[17].

Modulation bandwidth enhancement in the more desirable in-phase coherently coupled operation is presented in Fig. 11. Fig. 11 shows the small signal modulation response and optical spectrum with inset far-field intensity profile for a 1 $\times$ 2 phased photonic crystal VCSEL array with small signal modulation applied to element 2 and DC bias of $I_1 = 7.2$ mA and $I_2 = 7.1$ mA. The modulation bandwidth of 37 GHz is demonstrated while the array operates in the in-phase coupled mode, as shown by the on-axis peak in far-field intensity profile and inter-element lobe in near-field intensity profile (not shown). At this bias condition the emission gives 2.9mW of output power and is

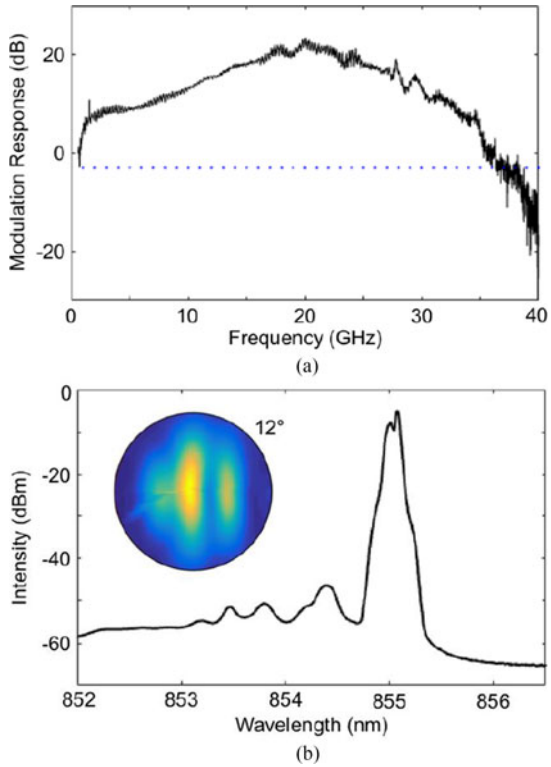

Fig. 11. (a) Small signal modulation response and (b) optical spectrum with inset far-field intensity profile for 1×2 phased VCSEL array (hexagonal lattice with $b = 2.7\,\mu$m and $b/a = 0.6$) with small signal modulation applied to Element 2 and DC bias of $I_1 = 7.2$ mA and $I_2 = 7.1$ mA.

highly single-mode with a side-mode suppression ratio (SMSR) of 40 dB as shown in Fig. 11.

VI. Conclusion

In conclusion, we have analyzed two-element phased VCSEL arrays from the perspective of monolithic injection locking and have incorporated the phase difference between the elements which arise for the supermode array emission. Our modeling indicates the phase between elements and the injection ratio are critical parameters that influence the modulation bandwidth. We have also reported on the design and fabrication of photonic crystal ion-implanted VCSEL arrays that can be tuned to coherence . From the coherent near- and far-fields we extract the relative phase and find qualitative agreement with our experimental observations. Significant modulation enhancement to >30 GHz is obtained for both in-phase and out-of-phase supermode operation. From our theory we can expect that designs that induce asymmetric field injection under injection-locked coherent operation should lead to further improvements. Therefore coherently coupled VCSEL arrays may enable significant modulation enhancement, perhaps leading to 100 Gb/s data rate from direct modulation of semiconductor lasers.

References

[1] M. B. Spencer and W. E. Lamb, "Theory of two coupled lasers," *Phys. Rev. A*, vol. 5, no. 2, pp. 893–898, Feb. 1972.

[2] R. Lang and K. Kobayashi, "External optical feedback effects on semiconductor injection laser properties," *IEEE J. Quantum Electron.*, vol. 16, no. 3, pp. 347–355, Mar. 1980.

[3] J. K. Butler, D. E. Ackley, and D. Botez, "Coupled-mode analysis of phase-locked injection laser arrays," *Appl. Phys. Lett.*, vol. 44, no. 3, pp. 293–295, Feb. 1984.

[4] E. Kapon, J. Katz, and A. Yariv, "Supermode analysis of phase-locked arrays of semiconductor lasers," *Opt. Lett.*, vol. 9, no. 4, pp. 125–127, Apr. 1984.

[5] H. Li, T. L. Lucas, J. G. McInerney, M. W. Wright, and R. A. Morgan, "Injection locking dynamics of vertical cavity semiconductor lasers under conventional and phase conjugate injection," *IEEE J. Quantum Electron.*, vol. 32, no. 2, pp. 227–235, Feb. 1996.

[6] C.-H. Chang, L. Chrostowski, and C. J. Chang-Hasnain, "Injection locking of VCSELs," *IEEE J. Sel. Topics Quantum Electron.*, vol. 9, no. 5, pp. 1386–1393, Sep. 2003.

[7] L. Chrostowski *et al.*, "50-GHz optically injection-locked 1.55-μm VCSELs," *IEEE Photon. Technol. Lett.*, vol. 18, no. 2, pp. 367–369, Jan. 2006.

[8] A. Hayat *et al.*, "Long wavelength VCSEL-by-VCSEL optical injection locking," *IEEE Trans. Microw. Theory Technol.*, vol. 57, no. 7, pp. 1850–1858, Jul. 2009.

[9] A. Hurtado, D. Labukhin, I. D. Henning, and M. J. Adams, "Injection locking bandwidth in 1550-nm VCSELs subject to parallel and orthogonal optical injection," *IEEE J. Sel. Topics Quantum Electron.*, vol. 15, no. 3, pp. 585–593, May/Jun. 2009.

[10] G. Hergenhan, B. Lücke, and U. Brauch, "Coherent coupling of vertical-cavity surface-emitting laser arrays and efficient beam combining by diffractive optical elements: Concept and experimental verification," *Appl. Opt.*, vol. 42, no. 9, pp. 1667–1680, Mar. 2003.

[11] G. R. Hadley, "Modes of a two-dimensional phase-locked array of vertical-cavity surface-emitting lasers," *Opt. Lett.*, vol. 15, no. 21, pp. 1215–1217, Nov. 1990.

[12] A. C. Lehman, J. J. Raftery, A. J. Danner, P. O. Leisher, and K. D. Choquette, "Relative phase tuning of coupled defects in photonic crystal vertical-cavity surface-emitting lasers," *Appl. Phys. Lett.*, vol. 88, no. 2, pp. 021102-1–021102-3, Jan. 2006.

[13] A. C. Lehman, D. F. Siriani, and K. D. Choquette, "Two-dimensional electronic beam-steering with implant-defined coherent VCSEL arrays," *Electron. Lett.*, vol. 43, no. 22, pp. 1202–1203, 2007.

[14] D. Siriani and K. Choquette, "Electronically controlled two-dimensional steering of in-phase coherently coupled vertical-cavity laser arrays," *IEEE Photon. Technol. Lett.*, vol. 23, no. 3, pp. 167–169, Feb. 2011.

[15] H. Dalir and F. Koyama, "29 GHz directly modulated 980 nm vertical-cavity surface emitting lasers with bow-tie shape transverse coupled cavity," *Appl. Phys. Lett.*, vol. 103, no. 9, pp. 091109-1–091109-4, Aug. 2013.

[16] X. Gu *et al.*, "850 nm transverse-coupled-cavity vertical-cavity surface-emitting laser with direct modulation bandwidth of over 30 GHz," *Appl. Phys. Express*, vol. 8, no. 8, pp. 082702-1–082702-4, Aug. 2015.

[17] S. T. M. Fryslie, M. P. Tan, D. F. Siriani, M. T. Johnson, and K. D. Choquette, "37-GHz modulation via resonance tuning in single-mode coherent vertical-cavity laser arrays," *IEEE Photon. Technol. Lett.*, vol. 27, no. 4, pp. 415–418, Feb. 2015.

[18] S. T. M. Fryslie, M. T. Johnson, and K. D. Choquette, "Coherence tuning in optically coupled phased vertical cavity laser arrays," *IEEE J. Quantum Electron.*, vol. 51, no. 11, Nov. 2015, Art. no. 2600206.

[19] K. D. Choquette, K. L. Lear, R. P. Schneider, and K. M. Geib, "Cavity characteristics of selectively oxidized vertical-cavity lasers," *Appl. Phys. Lett.*, vol. 66, no. 25, pp. 3413–3415, Jun. 1995.

[20] M. P. Tan, A. M. Kasten, J. D. Sulkin, and K. D. Choquette, "Planar photonic crystal vertical-cavity surface-emitting lasers," *IEEE J. Sel. Topics Quantum Electron.*, vol. 19, no. 4, Jul./Aug. 2013, Art. no. 4900107.

[21] A. M. Kasten, M. P. Tan, J. D. Sulkin, P. O. Leisher, and K. D. Choquette, "Photonic crystal vertical cavity lasers with wavelength-independent single-mode behavior," *IEEE Photon. Technol. Lett.*, vol. 20, no. 23, pp. 2010–2012, Dec. 2008.

[22] A. J. Danner, J. C. Lee, J. J. Raftery, N. Yokouchi, and K. D. Choquette, "Coupled-defect photonic crystal vertical cavity surface emitting lasers," *Electron. Lett.*, vol. 39, no. 18, pp. 1323–1324, 2003.

[23] A. J. Danner, J. J. Raftery, P. O. Leisher, and K. D. Choquette, "Single mode photonic crystal vertical cavity lasers," *Appl. Phys. Lett.*, vol. 88, no. 9, pp. 091114-1–091114-3, Mar. 2006.

[24] J. J. Raftery *et al.*, "In-phase evanescent coupling of two-dimensional arrays of defect cavities in photonic crystal vertical cavity surface emitting lasers," *Appl. Phys. Lett.*, vol. 89, no. 8, pp. 081119-1–081119-3, 2006.

[25] D. F. Siriani *et al.*, "Mode control in photonic crystal vertical-cavity surface-emitting lasers and coherent arrays," *IEEE J. Sel. Topics Quantum Electron.*, vol. 15, no. 3, pp. 909–917, May/Jun. 2009.
[26] D. F. Siriani and K. D. Choquette, "Implant defined anti-guided vertical-cavity surface-emitting laser arrays," *IEEE J. Quantum Electron.*, vol. 47, no. 2, pp. 160–164, Feb. 2011.
[27] D. F. Siriani and K. D. Choquette, "In-phase, coherent photonic crystal vertical-cavity surface-emitting laser arrays with low divergence," *Electron. Lett.*, vol. 46, no. 10, pp. 712–713, 2010.
[28] Z. Gao *et al.*, "Bottom-emitting coherently coupled vertical cavity laser arrays," *IEEE Photon. Technol. Lett.*, vol. 28, no. 4, pp. 513–515, Feb. 2016.
[29] K. D. Choquette and K. M. Geib, "Fabrication and performance of vertical cavity surface emitting lasers," in *Vertical Cavity Surface Emitting Lasers*, C. W. Wilmsen, H. Temkin, L. A. Coldren, Eds. New York, NY, USA: Cambridge Univ. Press, 1999, pp. 193–232, Ch. 5.
[30] M. T. Johnson, D. F. Siriani, and K. D. Choquette, "High-Speed beam steering with phased vertical cavity laser arrays," *IEEE J. Sel. Topics Quantum Electron.*, vol. 19, no. 4, Jul. 2013, Art. no. 1701006.
[31] M. T. Johnson, D. F. Siriani, J. D. Sulkin, and K. D. Choquette, "Phase and coherence extraction from a phased vertical cavity laser array," *Appl. Phys. Lett.*, vol. 101, no. 3, pp. 031116-1–031116-3, 2012.
[32] Z. Gao, S. T. M. Fryslie, B. J. Thompson, P. S. Carney, and K. D. Choquette, "Parity-time symmetry in coherently coupled vertical cavity laser arrays," *Optica*, vol. 4, no. 3, pp. 323–329, Mar. 2017.
[33] R. Lang, "Injection locking properties of a semiconductor laser," *IEEE J. Quantum Electron.*, vol. JQE-18, no. 6, pp. 976–983, Jun. 1982.
[34] J. Horer and E. Patzak, "Large-signal analysis of all-optical wavelength conversion using two-mode injection-locking in semiconductor lasers," *IEEE J. Quantum Electron.*, vol. 33, no. 4, pp. 596–608, Apr. 1997.
[35] L. Chrostowski and W. Shi, "Monolithic injection-locked high-speed semiconductor ring lasers," *J. Light. Technol.*, vol. 26, no. 19, pp. 3355–3362, Oct. 2008.
[36] S. S. Wang and H. G. Winful, "Dynamics of phase-locked semiconductor laser arrays," *Appl. Phys. Lett.*, vol. 52, no. 21, pp. 1774–1776, 1988.
[37] E. Kapon, C. Lindsey, J. Katz, S. Margalit, and A. Yariv, "Coupling mechanism of gain-guided integrated semiconductor laser arrays," *Appl. Phys. Lett.*, vol. 44, no. 4, pp. 389–391, 1984.
[38] D. Botez, L. J. Mawst, and G. Peterson, "Resonant leaky-wave coupling in linear arrays of antiguides," *Electron. Lett.*, vol. 24, no. 21, pp. 1328–1330, 1988.
[39] J. Ohtsubo, *Semiconductor Lasers: Stability, Instability and Chaos*, vol. 111. Berlin, Germany: Springer, 2012.
[40] X. Wang, C. Xiong, and J. Luo, "Coupling coefficients evaluation of a directional coupler using gain guided and index antiguided fibers," *Opt. Commun.*, vol. 282, no. 3, pp. 382–386, 2009.
[41] J. Katz, E. Kapon, C. Lindsey, S. Margalit, and A. Yariv, "Coupling coefficient of gain-guided lasers," *Appl. Opt.*, vol. 23, no. 14, pp. 2231–2233, 1984.
[42] L. Chrostowski *et al.*, "40 GHz bandwidth and 64 GHz resonance frequency in injection-locked 1.55 μm VCSELs," *IEEE J. Sel. Topics Quantum Electron.*, vol. 13, no. 5, pp. 1200–1208, Sep./Oct. 2007.
[43] F. Mogensen, H. Olesen, and G. Jacobsen, "Locking conditions and stability properties for a semiconductor laser with external light injection," *IEEE J. Quantum Electron.*, vol. 21, no. 7, pp. 784–793, Jul. 1985.
[44] C. H. Henry, N. A. Olsson, and N. K. Dutta, "Locking range and stability of injection locked 1.54 μm InGaAsp semiconductor lasers," *IEEE J. Quantum Electron.*, vol. 21, no. 8, pp. 1152–1156, Aug. 1985.
[45] L. A. Coldren, S. W. Corzine, and M. L. Mashanovitch, *Diode Lasers and Photonic Integrated Circuits*, vol. 218. New York, NY, USA: Wiley, 2012.
[46] A. Murakami, K. Kawashima, and K. Atsuki, "Cavity resonance shift and bandwidth enhancement in semiconductor lasers with strong light injection," *IEEE J. Quantum Electron.*, vol. 39, no. 10, pp. 1196–1204, Oct. 2003.
[47] E. K. Lau, L. J. Wong, and M. C. Wu, "Enhanced modulation characteristics of optical injection-locked lasers: A tutorial," *IEEE J. Sel. Topics Quantum Electron.*, vol. 15, no. 3, pp. 618–633, May/Jun. 2009.
[48] T. B. Simpson, J. M. Liu, A. Gavrielides, V. Kovanis, and P. M. Alsing, "Period-doubling route to chaos in a semiconductor laser subject to optical injection," *Appl. Phys. Lett.*, vol. 64, no. 26, pp. 3539–3541, Jun. 1994.
[49] M. C. España-Boquera and A. Puerta-Notario, "Noise effects in injection locked lasers simulation: Phase jumps and associated spectral components," *Electron. Lett.*, vol. 32, no. 9, pp. 818–819, 1996.
[50] J. M. Liu, H. F. Chen, X. J. Meng, and T. B. Simpson, "Modulation bandwidth, noise, and stability of a semiconductor laser subject to strong injection locking," *IEEE Photon. Technol. Lett.*, vol. 9, no. 10, pp. 1325–1327, Oct. 1997.
[51] E. K. Lau, H.-K. Sung, and M. C. Wu, "Frequency response enhancement of optical injection-locked lasers," *IEEE J. Quantum Electron.*, vol. 44, no. 1, pp. 90–99, Jan. 2008.
[52] H. Dalir, A. Matsutani, M. Ahmed, A. Bakry, and F. Koyama, "High frequency modulation of transverse-coupled-cavity VCSELs for radio over fiber applications," *IEEE Photon. Technol. Lett.*, vol. 26, pp. 281–284, Feb. 2014.
[53] M. Ahmed, A. Bakry, M. S. Alghamdi, H. Dalir, and F. Koyama, "Enhancing the modulation bandwidth of VCSELs to the millimeter-waveband using strong transverse slow-light feedback," *Opt. Express*, vol. 23, pp. 15365–15371, Jun. 2015.

Stewart T. M. Fryslie (S'12) received the B.S. degrees in electrical and computer engineering and in physics with mathematics minor from the South Dakota School of Mines and Technology, Rapid City, SD, USA, in 2010, the M.S. degree in electrical and computer engineering from the University of Illinois at Urbana-Champaign, Champaign, IL, USA, in 2013, where he is working toward the Ph.D. degree.

He is currently working as a photonic device Engineer in Freedom Photonics in Santa Barbara, CA, USA. His current research interests include semiconductor lasers, microwave photonics, and planar lightwave circuits. He received the 2016 Gregory Stillman Semiconductor Research Award from the ECE Department at the University of Illinois Urbana-Champaign and is a 2016 IEEE Photonics Society Graduate Student Fellow.

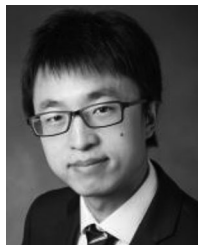

Zihe Gao (M'14) received the B.S. degree in physics from Nanjing University, Nanjing, China, in 2011, and the M.S. degree in physics from the University of Illinois at Urbana-Champaign, Champaign, IL, USA, in 2012. He is currently working toward the Ph.D. degree in electrical engineering at the University of Illinois at Urbana-Champaign. His research interests include lateral current injected membrane lasers and coherently coupled laser arrays.

Harshil Dave (M'15) received the B.S. degree in physics from Rutgers University, New Brunswick, NJ, USA, in 2014. He is currently working toward the Ph.D. degree in electrical engineering at the University of Illinois at Urbana-Champaign, Champaign, IL, USA. His main research interests include design, fabrication, and high speed modulation of injection locked photonic crystal VCSEL arrays.

Bradley J. Thompson (M'11) received the B.S. degree in electrical engineering with a minor in mathematics, and the M.S. degree from the University of Illinois at Urbana-Champaign, Champaign, IL, USA, in 2012 and 2015 respectively. He is working toward the Ph.D. degree with a focus on design, fabrication, and characterization of coherent VCSEL arrays.

Katherine Lakomy received the B.S degree in electrical engineering from the University of Maryland, College Park, MD, USA, in 2014. She is currently working toward the M.S degree in the same field at the University of Illinois Urbana-Champaign, Champaign, IL, USA and will continue on to work toward the Ph.D. degree. Her research interests include the fabrication of semiconductor devices, silicon photonics, and microcavity lasers.

Shiyun Lin received the M.S. and Ph.D. degrees in engineering science from Harvard University, Cambridge, MA, USA, in 2013. He is currently a Senior Hardware Engineer at Finisar Corp. Prior to this he was with Oracle in the Networking Group. His research interests include high-speed optical device design and testing, hybrid laser development for silicon photonics and optical interconnects. He has coauthored more than 40 papers in technical journals and conferences.

Patrick J. Decker (M'07) received the B.S. degree in applied physics with highest honors and the M.S. degree in electrical and computer engineering, both from Georgia Institute of Technology, Atlanta, GA, USA, in 2007 and 2008, respectively. While there from May 2007 to October 2010 and from May 2012 to May 2013, he was a Graduate Research Assistant in the Ultrafast Optical Communications Laboratory and 100 Gb/s Optical Networking Consortium, focusing on multimode optical communications. He focused on reducing the cost and complexity of optical interconnects while working as a Senior Design Engineer from October 2010 to January 2012 with the Applied Micro Circuits Corporation, Andover, MA, USA and worked on integration of mid-board optical modules into next-generation switches while at Oracle Corporation, San Diego, CA, USA, as a hardware Engineer from 2013 to January 2017. He is currently with Cisco Systems, Inc., San Jose, CA, USA, and is a member of the IEEE Photonics Society.

David K. McElfresh (M'77) received the B.S. degrees in electrical engineering and materials science and engineering and the M.S. and Ph.D. degrees in materials science from the University of California-Davis, Davis, CA, USA, in 1980 1982, and 1984, respectively. From 1984 to 1999 he held a variety of technical and technical management positions involving light emitting diode materials and products at Hewlett-Packard's Optoeletronics Division, San Jose, CA, USA. From 1999 to 2001, he was involved in research and development of new thermal inkjet pen technologies at Hewlett-Packard's Inkjet Research Laboratories, San Diego, CA, USA. In 2001, he joined SUN Microsystems (acquired by Oracle in 2010) and helped to establish their Physical Sciences Research Center in San Diego, CA, USA. He is a Director of Hardware Development and a Distinguished Engineer; leads and manages the Reliability Physics Group in the Systems Group that includes a state of the art characterization laboratory and advanced reliability testing and modeling technologies; and is a Principal Investigator for projects pursuing high speed, high reliability, low-power optical sources sponsored by Oracle Laboratory's External Research Office. He holds more than 50 U.S. patents.

José E. Schutt-Ainé (S'86–M'86–SM'98–F'07) received the B.S. degree in electrical engineering from the Massachusetts Institute of Technology, Cambridge, MA, USA, in 1981, and the M.S. and Ph.D. degrees from the University of Illinois at Urbana-Champaign (UIUC), Champaign, IL, USA, in 1984 and 1988, respectively. He joined the Hewlett-Packard Technology Center, Santa Rosa, CA, USA, as an Application Engineer, where he was involved in research on microwave transistors and high-frequency circuits. In 1983, he joined UIUC, and then joined the Electrical and Computer Engineering Department as a member of the Electromagnetics and Coordinated Science Laboratories, where he is currently involved in research on signal integrity for high-speed digital and high-frequency applications. He is a consultant for several corporations. His current research interests include the study of signal integrity and the generation of computer-aided design tools for high-speed digital systems. He received several research awards, including the 1991 National Science Foundation (NSF) MRI Award, the National Aeronautics and Space Administration Faculty Award for Research in 1992, the NSF MCAA Award in 1996, and the UIUC-National Center for Superconducting Applications Faculty Fellow Award in 2000. He is currently serving as Co-Editor-in-Chief of the IEEE TRANSACTIONS ON COMPONENTS, PACKAGING AND MANUFACTURING TECHNOLOGY.

Kent D. Choquette (M'97–F'03) received the B.S. degrees in engineering physics and applied mathematics from the University of Colorado-Boulder, Boulder, CO, USA, and the M.S. and Ph.D. degrees in materials science from the University of Wisconsin-Madison, Madison, WI, USA.

He held a postdoctoral appointment at AT&T Bell Laboratories, Murray Hill, NJ, USA and then joined Sandia National Laboratories in Albuquerque, NM, USA, working as a Principal Member of Staff from 1992 to 2000. In 2000, he joined the Electrical and Computer Engineering Department, University of Illinois and is currently the Able Bliss Professor of Engineering. He leads the Photonic Device Research Group which pursues the design, fabrication, characterization, and applications of semiconductor vertical cavity surface-emitting lasers, photonic crystal light sources, nanofabrication technologies, and hybrid integration techniques. He has authored more than 300 technical publications and five book chapters, and has presented numerous invited talks and tutorials at international conferences. He has served as an Associate Editor of the IEEE JOURNAL OF QUANTUM ELECTRONICS, IEEE PHOTONIC TECHNOLOGY LETTERS, and JOURNAL LIGHTWAVE TECHNOLOGY, as well as a Guest Editor of IEEE JOURNAL OF SELECTED TOPICS IN QUANTUM ELECTRONICS.

Dr. Choquette received the 2016 SPIE Technology Achievement award, the 2012 OSA Nick Holonyak Jr. Award, the 2008 IEEE Photonics Society Engineering Achievement Award, and from 2000 to 2002 he was a IEEE/LEOS Distinguished Lecturer. He is a Fellow of the Optical Society of America, a Fellow of SPIE, and a Fellow of the American Association for the Advancement of Science. He is currently the President of the IEEE Photonics Society during 2016-2017.